Published in final edited form as:
Neuroimage. 2007 November 1; 38(2): 271–279.

Multiparametric Magnetic Resonance Imaging Analysis of the Corticospinal Tract in Multiple Sclerosis

Daniel S. Reich, Ph.D.M.D.[1,2], **Seth A. Smith, Ph.D.**[2,4], **Kathleen M. Zackowski, Ph.D.**[1,3,5], **Eliza M. Gordon-Lipkin, B.S.**[1], **Craig K. Jones, Ph.D.**[2,4,6], **Jonathan A. D. Farrell, B.S.**[2,4], **Susumu Mori, Ph.D.**[2,4], **Peter C. M. van Zijl, Ph.D.**[2,4], and **Peter A. Calabresi, M.D.**[1]

1*Department of Neurology, Johns Hopkins University, 600 N Wolfe St, Baltimore, MD 21287*

2*Department of Radiology, Johns Hopkins University, 600 N Wolfe St, Baltimore, MD 21287*

3*Department of Physical Medicine and Rehabilitation, Johns Hopkins University, 600 N Wolfe St, Baltimore, MD 21287*

4*F. M. Kirby Research Center for Functional Brain Imaging, Kennedy Krieger Institute, 707 N Broadway, Baltimore, MD 21205*

5*Department of Physical Medicine and Rehabilitation, Kennedy Krieger Institute, 707 N Broadway, Baltimore, MD 21205*

Abstract

Background/purpose—Muscle weakness is an important feature of multiple sclerosis and is responsible for much of the disability associated with that condition. Here, we describe the quantitative magnetic resonance imaging (MRI) attributes of the major intracerebral motor pathways – the corticospinal tracts – in multiple sclerosis. To do so, we develop an intuitive method for creating and displaying spatially normalized tract-specific imaging data.

Methods—In 75 individuals with multiple sclerosis and 29 healthy controls, the corticospinal tracts were reconstructed from diffusion tensor imaging at 3 Tesla. Multiple MRI indices – T2 relaxation time; fractional anisotropy; mean, longitudinal, and transverse diffusivity; and magnetization transfer ratio – were examined within the reconstructed tracts. Spatially normalized tract profiles were created to compare, across subjects, the variation in MRI index as a function of tract position.

Results—Each index's tract profile had a characteristic shape. Individual subjects had markedly abnormal tract profiles, particularly at lesion sites. On average, tract profiles were different between patients and controls, particularly in the subcortical white matter and corona radiata, for all indices examined except for fractional anisotropy. Magnetization transfer ratio was further decreased in subjects with secondary progressive disease. Tract asymmetry was increased in multiple sclerosis compared to controls.

Correspondence should be addressed to Daniel S. Reich, M.D., Ph.D., 600 N Wolfe St / Phipps B-112, Baltimore, MD 21287. Tel: 410-502-0012. reichd@jhmi.edu..

6Current address: Imaging Labs, Robarts Research Institute, PO Box 5015, 100 Perth Drive, London, ON N6A 5K8, Canada

Prior presentation: Portions of this work were presented at the 2006 annual meeting of the American Neurological Association (Chicago, Illinois; October 8–11, 2006).

Conclusion—Multiparametric MRI allows rapid detection, localization, and characterization of tract-specific abnormalities in multiple sclerosis. Tract profiles bridge the gap between whole-brain imaging of neurological disease and the interrogation of individual, functionally relevant subsystems.

Keywords

multiple sclerosis; corticospinal tract; pyramidal tract; diffusion tensor imaging; magnetization transfer imaging; tract profiles

Introduction

Multiple sclerosis (MS) is a central nervous system disorder, with protean manifestations and multiple subtypes, that can lead to a wide spectrum and degree of disability. Among the functional systems that it frequently affects is the pyramidal motor system, resulting in weakness of one or more limbs or the facial muscles. Abnormalities in this system contribute to Kurtzke's Expanded Disability Status Score (EDSS) (Kurtzke, 1983) and can result in clinically relevant disability. Because both its function and location within the brain are well defined, the pyramidal system serves as a model for the detection and clinicoradiologic assessment of functional disability in MS.

In this paper, we discuss the magnetic resonance imaging (MRI) characteristics of a major portion of the pyramidal system, the corticospinal tract (CST), in MS. In doing so, we have two primary objectives: (1) to facilitate the detection and monitoring of CST-specific abnormalities in individual patients; and (2) within an MS cohort, to assess the typical degree and locations of those abnormalities. In the first instance, we hope to be able to evaluate objectively the state of an individual's disease and ultimately to monitor its progression over time, or, hopefully, its recovery after specific therapy. In the second instance, we expect to gain a deeper understanding of the ways in which MS can affect the motor system and ultimately to track the effects of novel therapeutic agents on a population level.

The imaging appearance of the CST in MS has been studied previously, although not over its entire intracranial course or for a wide variety of MRI indices in the same subject. MS plaques can affect the CST, causing typical changes of increased T2-weighted signal, decreased T1-weighted signal, and enhancement following contrast administration. Even in the portions of the CST that are not overtly affected by MS plaques, there are MRI abnormalities including increased T2-weighted signal, which has been interpreted to reflect Wallerian degeneration (Simon et al., 2000). With diffusion tensor imaging (DTI), a newer quantitative MRI technique, MS plaques typically demonstrate increased mean diffusivity (MD) and decreased fractional anisotropy (FA) (Tievsky et al., 1999; Werring et al., 1999). Similar abnormalities have also been reported along the CST specifically (Lin et al., 2007; Wilson et al., 2003). Additionally, levels of N-acetyl aspartate, a measure of axonal integrity, are decreased within the internal capsule, through which the CST passes (Lee et al., 2000). However, the degree to which these MRI abnormalities relate to axonal pathology along the CST remains unclear (DeLuca et al., 2004).

MRI abnormalities along the CST have also been studied in other neurological diseases. In neuromyelitis optica, a neuroimmunological disorder related to MS, decreased FA and increased MD have been observed in the cerebral peduncles (Lin et al., 2006). Similar patterns have been described in other neurological diseases, including stroke (Werring et al., 2000) and amyotrophic lateral sclerosis (Toosy et al., 2003). In the latter, the magnetization transfer ratio (MTR), which is influenced by protons bound to macromolecules such as myelin, has been reported to be decreased in the CST but not in nearby white matter (Tanabe et al., 1998).

In this paper, we use DTI with fiber tracking (Mori et al., 1999; Mori and van Zijl, 2002; Mori et al., 2005) to identify the intracerebral portion of the CST. This technique, while still in relative infancy and not in general clinical use, is emerging as a powerful tool for assessing pathway-specific abnormalities in neurological disease. Within the identified tracts, we measure various quantitative MRI indices derived from DTI and additional acquisitions (T2 and magnetization transfer) that are anatomically coregistered to the DTI data. We calculate each index as a function of position within the tract, referring to plots depicting their spatial variation as "tract profiles." Tract profiles allow localization of focal tract abnormalities in individual subjects. We also consider the asymmetry between the right and left tracts.

This study builds upon previous work (Reich et al., 2006) that describes our methods for identifying, characterizing, and detecting asymmetry within the CSTs of healthy volunteers. The present study includes data from those healthy subjects as well as additional control data that were obtained after the first study was completed. In this paper, we focus on the presentation and discussion of data from our subjects with MS.

Materials and Methods

Magnetic resonance imaging

We studied 75 individuals with MS: 43 individuals with relapsing remitting MS (RRMS; median age: 40; range: 24 – 60; 30 women and 10 men); 22 individuals with secondary progressive MS (SPMS; median age: 50; range: 40 – 67; 13 women and 9 men); and 10 individuals with primary progressive MS (PPMS; median age: 54; range: 44 – 67; 6 women and 4 men). We also studied 29 healthy controls (median age: 33; range: 22 – 63; 20 women and 9 men). All imaging protocols were accepted by the Institutional Review Boards at Johns Hopkins University and the Kennedy Krieger Institute, where scanning was done, and subjects were required to document their informed consent to participate in the study.

Imaging was done on a 3 Tesla MRI scanner (Philips Medical Systems, Best, The Netherlands). A full description of our scanning protocol, as well as detailed results form our cohort of healthy volunteers, can be found in a previous publication (Reich et al., 2006). Note that the control data used in the present study include those subjects as well as 9 additional subjects who were scanned after the original study was submitted for publication.

DTI on all subjects used spin echo, single shot, echo planar imaging and a sensitivity encoding (SENSE) reduction factor of 2.5. We obtained axial diffusion weighted images in 32 non-coplanar gradient directions with a nominal *b*-value of 700 s/mm^2. We also obtained a scanner average of 5 minimally diffusion weighted scans with $b \approx 33$ s/mm^2. We collected data in isotropic 2.2 mm voxels, reconstructing to an in-plane resolution of 0.83 mm, and covered nearly the entire brain from the cervicomedullary junction to just below the vertex. We repeated the 3 min 38 sec sequence twice to improve the signal-to-noise ratio, and all data were used in the tensor calculation.

We coregistered all images (from the DTI acquisitions as well as from the other acquisitions described below) to the first minimally diffusion-weighted scan using the Automatic Image Registration (AIR) algorithm (Woods et al., 1992) with a 6-parameter rigid-body transformation, and we corrected the gradient directions for the rotational component of the transformation. We then estimated the diffusion tensor in the standard fashion (Basser et al., 1994) and calculated maps of fractional anisotropy (FA), mean diffusivity (MD), longitudinal diffusivity ($\lambda_{\|}$), and transverse diffusivity ($\lambda_{\perp}$) (Basser and Pierpaoli, 1996). ($\lambda_{\|}$ corresponds to diffusion parallel to the long axis of a fiber bundle and $\lambda_{\perp}$ to diffusion perpendicular to that axis.) We also created color coded maps from the principal eigenvectors, weighted by the fractional anisotropy (Pajevic and Pierpaoli, 1999). These analyses were performed in

DtiStudio (Jiang et al., 2006), as well as with custom software purpose-written in Matlab (The Mathworks, Natick, MA).

Additional MRI acquisitions were obtained on subsets of the subjects scanned with DTI as the full protocol could not be obtained on every subject due to scanning time constraints and subject discomfort. On 66 individuals with MS and 26 controls, we acquired axial, double echo, turbo spin echo scans (TR=4158 ms; 3 min 27 sec) to visualize proton density (TE=28.2 ms) and T2 weighted (TE=80 ms) images, and to estimate absolute T2 relaxation time. From 63 subjects with MS and 24 controls, we acquired echo planar axial 3D spoiled gradient echo images, with and without 1.5 kHz off-resonance preparation, for the calculation of MTR (TR=65 ms, TE=15 ms, 3 repeats, 1 min 41 sec each) (Smith et al., 2006). Further scan details are provided elsewhere (Reich et al., 2006).

Fiber tracking

We used the DTI datasets to obtain 3D reconstructions of the CSTs using the fiber association by continuous tractography (FACT) method (Mori et al., 1999; Mori and van Zijl, 2002; Mori et al., 2005). Briefly, tracts were reconstructed using FA and the principal eigenvector of the diffusion tensor. Whole-brain seeding was used with predefined thresholds of FA and principal eigenvector turning angle (0.13 and 40 degrees, respectively). The relatively low FA cutoff is permissive in that it fails to reject many spurious fibers, but the choice is necessary because FA is typically decreased within MS plaques (Tievsky et al., 1999; Werring et al., 1999), and we wanted to be able to track through those plaques to the extent possible.

To compensate for this choice and to reject spurious fibers, we chose multiple restrictive ROIs to limit the reconstructed CSTs to their known anatomical course, as described in a previous publication (Reich et al., 2006). One of us (DSR) drew axial ROIs around the entire caudal medulla; the ipsilateral anterior pons; and the ipsilateral cerebral hemisphere at the level of the subcortical white matter. We selected for further analysis the fibers that passed through all of these ROIs, traversing the entire intracranial CST from the cortex to the medulla. Rare spurious fibers passing through the contralateral anterior and bilateral posterior pons, and other fibers that clearly fell outside the major portion of the CST, were then manually excluded.

Tract profiles

We used tract profiles to depict the variation in each MRI index (FA, MD, $\lambda_{||}$, $\lambda_{\perp}$, MTR, and T2) as a function of location along the CST. This was done simply by plotting the mean of the index, within a specified spatial window, against the axial slice number (a convenient choice for the CST, which generally runs perpendicular to the axial plane). In order to determine how a given subject compares to other subjects, we applied a spatial normalization procedure to the tract profiles. Such a normalization is necessary because brain and tract shape change from one person to the next, so that axial scan positions were not constant across subjects.

The spatial normalization proceeded as follows. We divided each CST into six segments of approximately equal length according to anatomical landmarks defined on axial MRI sections of the color-coded principal eigenvector maps. These six segments correspond approximately to the subcortical white matter, corona radiata, internal capsule, midbrain, pons, and medulla, which are denoted by abbreviations in the figures. Due to inconsistencies in defining the imaging volume across subjects, data from the medulla were only obtained for 56 (75%) of the subjects with MS and 18 (62%) of the controls.

The seven boundary points of the six segments of the CST are illustrated in Figure 1. Each of the segments was approximately 2 cm long, with a wide range of variation. Segments were then divided into 20 equal subsegments, each about 1 mm long. MRI indices were boxcar

averaged within a sliding window 4 subsegments wide and then plotted against subsegment number to obtain the tract profile. Profiles from each subject were compared to the average profile obtained from controls.

Tract profile statistics

Within each segment of the CST, and across the entire tract, we compared median MRI indices between subjects with MS and controls using multiple linear regression analysis, accounting for the contributions made by age, sex, and number of reconstructed fibers per tract. Subject group and sex were considered categorical variables in the regression model, whereas age and number of reconstructed fibers were considered continuous variables. The significance level for each variable is the *p*-value that corresponds to the partial Pearson correlation coefficient for that variable, holding the other variables constant. Statistical analyses were performed in Stata (StataCorp LP, College Station, TX).

To assess whether a particular median MRI index within any segment or across the entire tract was abnormal, we compared that index to the distribution obtained from controls. For this purpose, we used repeated results from the controls if more than one scan was available. The number of scans per control was as follows: 1 scan (n=15); 2 scans (n=9); 3 scans (n=4); 4 scans (n=1). In order to avoid bias due to repeated measurements from the same individual, results from subjects scanned more than once were weighted by the inverse of the number of scans for that subject (Taylor et al., 1996). A result was considered abnormal if it was below the 5th or above the 95th percentile of results from controls. Every individual contributed two tracts, from the left and right CSTs, so the number of indices in each control distribution was twice the number of individuals. Because of the exploratory nature of this work, we made no specific correction for multiple comparisons, and we simply report significance as *p* values.

Asymmetry analysis

To quantify the differences between the right and left CSTs, we used an asymmetry index, described in a previous publication (Reich et al., 2006), and defined (for the j^{th} subsegment) as:

$$A_j = \frac{I_{R,j} - I_{L,j}}{I_{R,j} + I_{L,j}},$$

where $I_{R,j}$ is the index of interest derived from the j^{th} subsegment of the right CST and $I_{L,j}$ the corresponding index from the j^{th} subsegment of the left CST. A_j can range from −1 (maximum asymmetry with the index on the right equal to 0) to 1 (maximum asymmetry with the index on the left equal to 0); A_j=0 corresponds to equality between the indices on the two sides. Total tract asymmetry was defined as the root mean square asymmetry across the entire tract, $\sqrt{\langle A_j^2 \rangle}$, and ranges from 0 to 1. We assessed the significance of tract asymmetry by the procedures described in the previous paragraph, comparing the observed asymmetry value to the distribution obtained from healthy controls.

Results

Sample tract profiles

We found a range of abnormalities in the CSTs of individuals with MS, as illustrated in Figure 2 for three representative examples. Each example highlights abnormalities in one or two of the MRI indices. The first subject (panel A) is a 41-year-old woman with RRMS with no clinical weakness on either side. Her MRI reveals many confluent areas of T2-weighted signal abnormality, some of which are seen in the FLAIR image. She had no lesions that enhanced with gadolinium at the time of examination. Both CSTs pass through areas of T2-weighted

hyperintensity as they traverse the periventricular white matter. These areas correspond to loci of increased transverse diffusivity ($\lambda_\perp$; second image, panel A). Bilaterally increased $\lambda_\perp$ is seen to better advantage in the tract profile (graph, panel A), which shows the variation in that index as a function of normalized distance along the tract. The area of greatest abnormality (red arrow) is in the periventricular white matter, which is a typical site of MS plaques.

The images in panel B come from a 32-year-old woman with RRMS with bilateral extremity weakness. This individual has multi-level tract abnormalities. In the top row of panel B, FLAIR and MTR images through the brainstem are shown, together with the MTR tract profile; in the bottom row of panel B, the second image and tract profile depict mean diffusivity (MD). There is an area of focally decreased MTR in the right midbrain (dashed arrow) as well as a long segment of decreased MTR in the corona radiata and subcortical white matter. MD is normal at the level of the midbrain and focally abnormal at the junction of the corona radiata and subcortical white matter (solid arrow).

Panel C shows data from a 52-year-old man with PPMS, manifested primarily by spasticity and impaired ambulation. His MRI reveals marked periventricular signal abnormality without evidence of enhancement following gadolinium administration. In the corona radiata, we find a segment of elevated FA (arrow), more on the right than on the left. This elevation is due to increased longitudinal diffusivity ($\lambda_{||}$; bottom row) with normal or minimally decreased transverse diffusivity ($\lambda_\perp$; not shown). Unchanged or even mildly elevated FA in this region is a common and somewhat surprising finding in our subjects, which is addressed further in the Discussion.

Average tract profiles

Just as it enables rapid determination of the portions of the CST that are abnormal in each individual with MS, the tract profile analysis also reveals patterns of abnormality across our cohort of subjects with MS. This is shown in Figure 3, in which average tract profiles from subjects with MS are compared to average tract profiles from controls. Across the entire tract, there are significant differences in MD, $\lambda_{||}$, $\lambda_\perp$, and MTR. The difference between subjects with MS and controls is most pronounced in the periventricular zone – which includes portions of the segments labeled as subcortical white matter and corona radiata – where, on average, MS patients have significantly elevated MD, $\lambda_{||}$, $\lambda_\perp$, and absolute T2, and significantly decreased MTR. The region of elevated $\lambda_{||}$ is more diffuse than the region of elevated $\lambda_\perp$. Perhaps surprisingly, FA is not significantly decreased in the MS CST.

Overall, we find very few significant differences among average tract profiles for the three MS subtypes. This is illustrated, for RRMS and SPMS, in Figure 4; differences are even smaller for the other pairwise group comparisons. Although there is a barely significant difference between the two groups for MD across the entire CST, the most prominent finding is lower MTR in the internal capsule and midbrain in SPMS. MTR in this portion of the tract is slightly decreased in all subjects with MS compared to controls (Figure 3), but not significantly so. Notably, however, there are no significant subgroup differences in the periventricular zone, where most of the abnormalities that distinguish subjects with MS from controls are found.

Abnormality of individual tract profiles

Figure 5A demonstrates that between 20% and 50% of MS CSTs were significantly abnormal for each MRI index except for FA, where the percentage was close to the 5% expected by chance alone. Normal cutoffs were derived nonparametrically from the control data as described in Methods. Note that the size of our control population did not allow us to control this analysis for age, sex, or number of reconstructed fibers, unlike the group analysis of Figures 3 and 4. As for the group results, most of the abnormalities were in the periventricular zone,

but a substantial number of subjects had decreased MTR and elevated MD more distally along the tract.

Asymmetry

MS is an asymmetric disorder, typically affecting both sides of the brain and spinal cord, but in different ways and to different extents. To test the hypothesis that the disease can disrupt the structural symmetry between the right and left sides of the brain, we calculated a total tract asymmetry index as described in Methods. This index ranges from 0 (symmetry) to 1 (maximal asymmetry). Overall, median asymmetry was low, ranging from 0.02 to 0.09 in MS (Figure 5B). Multi-way ANOVA, controlling for age, sex, and average number of reconstructed fibers across the two tracts, demonstrates significantly increased tract asymmetry in MS for $\lambda_{\perp}$ (p=0.004), T2 (p=0.01), and MTR (p=0.004), but not for FA, MD, or $\lambda_{||}$. Figure 5C demonstrates that, except for $\lambda_{||}$, between 20% and 50% of subjects with MS had significantly asymmetric tract indices compared to the distribution of controls.

Discussion

Our multiparametric analysis of the values of 6 MRI indices within the corticospinal tracts of a cohort of subjects with MS and healthy controls reveals significant abnormalities in individuals and, across the population, typical areas of abnormality within the tract. Our work also represents, to our knowledge, the most comprehensive, quantitative description of the range of MRI abnormalities found in a specific functional system within the brains of MS patients. We examined the CSTs because of their functional importance, the ease with which their courses are reconstructed with DTI, and the ability to obtain a clinical assessment of their dysfunction. Due to the methodological issues involved in accurately characterizing clinical dysfunction and comparing that dysfunction with imaging abnormalities, we defer analysis of the relationship between MRI findings and motor weakness to future work.

Tract profiles

The most useful methodological contribution of this work is in the development of spatially normalized tract profiles that depict the variation in MRI indices as a function of position along a tract of interest, in this case the CST. By interpolating between anatomically well defined boundary points within the tract – identified separately in each individual – we achieve a one-to-one correspondence among tract positions in different individuals, or in different scans of the same individual. This enables a quantitative description of the normal range of variation of MRI indices, parametric in tract position. An individual's deviation from this normal range, as well as the location of any abnormalities, become readily apparent in plots such as those of Figure 2. Because tract profiles for each index have characteristic shapes, averaging MRI indices across the whole tract is likely to have only limited utility.

Although plots of MRI index vs. tract position have been published (Lin et al., 2006; Partridge et al., 2005; Stieltjes et al., 2001; Virta et al., 1999; Xue et al., 1999), to our knowledge no prior study covers as many indices over as long a section of the CST. Since it is unlikely that any single MRI index has a unique pathological correlate (e.g., demyelination vs. axonal disruption), the ability to examine multiple MRI indices simultaneously is an important step in acquiring a more complete description of the damage done to brain tissue by neurological disease. Accomplishing this with limited scan times requires high field MRI scanners and sequence optimization. In this vein, it is worth noting that the scans described here – a single double echo T2 sequence, 2 repeats of the DTI, and 3 repeats of the MT – require 16 minutes of scan time at 3T. (Repeated acquisitions may not be strictly necessary, although for this analysis we used all available data.) The protocol can therefore be used to examine patients on a routine basis, as well as in the context of clinical trials.

The method of tract profile normalization that we describe is not unique, although it is rapid, efficient and, as we have shown, able to detect abnormalities in MS. Other methods might prove more useful, for example, when dealing with tracts where natural segment boundaries are more difficult to define. One alternative method could involve coregistration of the DTI dataset from each subject to an appropriate atlas, which could be accomplished through any number of published methods (Jones et al., 2002; Xu et al., 2003). General methods of tract warping, taking into account curvatures and torsions, have also been explored (Batchelor et al., 2006), although not specifically in the context of tract profiles. A probabilistic tracking method has been applied to the pyramidal tracts of patients with clinically isolated syndromes suggestive of MS, revealing changes in diffusivity without significant changes in FA (Pagani et al., 2005). However, such probabilistic methods may be limited by distortions in overall brain architecture induced by disease. Regardless, it is likely that optimizing the coregistration process will tighten the normal range of tract profiles and thus increase sensitivity for detection of abnormality in disease, both within individuals and across populations.

Average vs. individual tract profiles

It is important to realize that because MS affects different individuals in different ways, the average tract profiles shown in Figure 3 are artificial constructions. They are very useful for detecting the locations along the tract that tend to be abnormal in MS; for the CST, these locations are the subcortical white matter and corona radiata for most indices and nearly the entire brain for MTR, particularly in SPMS. Where a lesion is present in an individual, the tract profile will be much more abnormal than the average MS tract at that location, as demonstrated in Figure 2. Thus, average profiles underestimate the degree of tract involvement by including relatively unaffected tracts and by blurring the tract profiles of individuals with lesions at different locations along the tract.

A related issue involves the distinction between MS lesions and the so-called “normal appearing white matter,” which has been demonstrated in many studies to be subtly abnormal in MS (Evangelou et al., 2000; Loevner et al., 1995; Werring et al., 1999). The tract profiles in our study do not distinguish between these different tissue types, but visual inspection suggests that most of the abnormalities that fall outside the normal range are due to lesions. It would be possible, with careful tissue segmentation, to construct separate profiles for lesional and normal appearing tissue, and such an exercise is likely to be informative.

Individual MRI indices

For most of the MRI indices discussed here, the direction of change in CST profiles of MS patients, reflected in the average profiles of Figure 3, parallels the direction of change for that index within MS plaques and also within so-called “normal-appearing” white and gray matter. Thus, we find increased MD (Tievsky et al., 1999;Werring et al., 1999), increased T2, and decreased MTR (Dousset et al., 1992). FA does not conform to this pattern and is discussed further below.

Values of selected DTI indices (most commonly, MD and FA) along the CST have been reported in a previous study that used regions of interest at various axial positions (Toosy et al., 2003), with results in healthy controls similar to those reported here. A previous publication from our group demonstrates differences in multiple MRI indices in the hemispheric vs. brainstem portions of the CST (Reich et al., 2006). In MS, tract-specific analysis of the CST, using DTI, has demonstrated increased MD and mildly decreased FA along the tract, although indices as a function of tract position were not reported (Wilson et al., 2003).

Over a more restricted segment of the CST and set of MRI indices, tract profiles with similar shapes to those described here were found in subjects with neuromyelitis optica (NMO) and

in healthy controls (Lin et al., 2006). However, we did not find that subjects with MS had decreased FA, increased MD, or $\lambda_{\perp}$ within the cerebral peduncles, as was found in NMO. Whether this is due to differences between MS and NMO, or to technical differences between the two studies (e.g., 3T vs. 1.5T MRI scanner and 32 vs. 6 diffusion gradients), remains to be determined.

We find that MTR is the MRI index for which the overall tract profile is abnormal in the greatest number of individuals with MS (36%). MTR has long been known to be a sensitive MRI marker of MS-related pathology (Dousset et al., 1992; Filippi and Rocca, 2004). In our results, average MTR is diminished over nearly the entire course of the intracranial CST, although the difference only achieves statistical significance in the rostral portion of the tract. In MS, MTR is sensitive to damage to both axons (van Waesberghe et al., 1999) and myelin, with perhaps a greater relative contribution from myelin (Schmierer et al., 2004). Our finding that MTR is significantly lower in subjects with progressive compared to relapsing MS (Figure 4) is consistent with the notion that MTR is affected by factors other than demyelination – although demyelination is prominent even in PPMS (Lucchinetti et al., 2000).

Although FA within MS plaques and normal-appearing white matter has been shown to be decreased relative to control populations (Tievsky et al., 1999; Werring et al., 1999), we find, on average, no significant differences along the CST. In some cases (see Figure 2C), FA is slightly elevated in the corona radiata and internal capsule, and this trend is also visible in the average tract profiles of Figure 3. Within individual plaques, we find that FA is decreased as expected (not shown), although not to the same extent that MD and the directional diffusivities are increased, or that MTR is decreased.

Unchanged FA in the CST – particularly in the regions where there are significant changes in MD, T2, and MTR – seems at first surprising, but it is best explained on technical grounds. FA is a measure of the degree to which the 3D probability density function of water diffusion within a single voxel is oblong (FA closer to 1) or spherical (FA closer to 0). Even under normal circumstances, the measured FA is expected to decrease where local tract curvature is high relative to voxel size. At those sites, each voxel contains axons that are turning sharply, which leads to a more spherical shape of the diffusion probability density function and therefore a lower FA. The periventricular zone, in which MRI indices are most abnormal in MS, is close to the point of highest tract curvature, where the fibers of the CST converge to enter the internal capsule. Thus, the primary determinant of FA in this region is probably tract curvature, which dominates effects due to disease. Indeed, under some circumstances, FA might even increase in these regions in MS – if, for example, there is a decrease in local tract curvature due to brain atrophy, a prominent result of MS (Rudick et al., 1999).

Our results indicate that mean diffusivity (MD), as well as its longitudinal ($\lambda_{||}$) and transverse ($\lambda_{\perp}$) components, are on average increased in MS, with the abnormality in $\lambda_{||}$ extending over a longer segment of the tract. (By itself, a region of elevated $\lambda_{||}$ with unchanged $\lambda_{\perp}$ would yield increased FA.) As with other MRI index abnormalities, increased diffusivity is most prominent in the corona radiata and subcortical white matter. Within MS plaques (see Figure 2), diffusivity can be markedly increased, consistent with multiple previous reports (Tievsky et al., 1999;Werring et al., 1999).

Asymmetry

Tract asymmetry indices comparing the right and left CST profiles are increased in MS relative to controls (Figure 5B–C) but are still overall close to their minimum value of 0. Increased asymmetry reflects the fact that MS is for the most part a patchy disease, despite multiple findings of MRI abnormalities in the so-called normal appearing white matter. In practice, however, little additional information is gained by considering asymmetry in addition to the

values of the MRI indices themselves. Moreover, decreasing asymmetry was not associated with chronic, progressive disease, as might perhaps be expected (data not shown).

Limitations

Our statistical analysis included no corrections for multiple comparisons, primarily because the goal of this study was to explore the value of tract profile analysis and to determine the MRI indices that are most abnormal along the CST in MS. Needless to say, future projects that use these methods in the context of longitudinal studies or clinical trials will need to pay close attention to this issue. In addition, the control population was relatively small and had some differences in baseline characteristics – particularly, younger age – from the MS cohort. Our group analysis partially controls for age differences, which can have a substantial impact on DTI indices (Jones et al., 2006).

Another limitation of our analysis is that coregistration of DTI images with images from other sequences, including MT and T2, is imperfect in certain regions of the brain. Visual inspection indicates that for the CST, the area most strongly affected is the medulla, which probably accounts for some of the variability observed in the tract profiles in that region on the T2 scans (see Figure 3). Distortions were similar for the DTI and MT datasets because both used echo planar readout schemes. Coregistration in the periventricular zones did not present a problem. Finally, the tractography method leads to substantial variability in the number of reconstructed fibers, which can also affect the measured MRI indices. More robust and automated fiber tracking methods would help to alleviate this problem.

Conclusion

The magnetic resonance imaging appearance of the corticospinal tracts in multiple sclerosis is abnormal both within individuals and across the MS population. Spatially normalized tract profiles allow easy identification of the location of those abnormalities and offer the possibility of specific, quantitative assessment of individual functional systems in the brain. Future work will examine the correlations between tract-specific abnormalities and functional disability.

Acknowledgements

We thank Terri Brawner, Karen DeBusk, Prachi Dubey, Kathleen Kahl, Ivana Kusevic, Mathew Pulicken, and Setsu Wakana for their assistance with this project.

Grant support: National Multiple Sclerosis Society Collaborative Center Award; National Multiple Sclerosis Society TR-3760-A-3 (PC); NIH RR15241, RO1EB3543, AG20012, and EB000991 (SS, CJ, PVZ, SM); the Nancy Davis Center without Walls (PC); and Philips Medical Systems (CJ). Dr. van Zijl is a paid lecturer for Philips Medical Systems, an arrangement that has been approved by Johns Hopkins University in accordance with its conflict of interest policies.

References

Basser PJ, Mattiello J, LeBihan D. Estimation of the effective self-diffusion tensor from the NMR spin echo. J Magn Reson B 1994;103:247–254. [PubMed: 8019776]

Basser PJ, Pierpaoli C. Microstructural and physiological features of tissues elucidated by quantitative-diffusion-tensor MRI. J Magn Reson B 1996;111:209–219. [PubMed: 8661285]

Batchelor PG, Calamante F, Tournier JD, Atkinson D, Hill DL, Connelly A. Quantification of the shape of fiber tracts. Magn Reson Med 2006;55:894–903. [PubMed: 16526017]

DeLuca GC, Ebers GC, Esiri MM. Axonal loss in multiple sclerosis: a pathological survey of the corticospinal and sensory tracts. Brain 2004;127:1009–1018. [PubMed: 15047586]

Dousset V, Grossman RI, Ramer KN, Schnall MD, Young LH, Gonzalez-Scarano F, Lavi E, Cohen JA. Experimental allergic encephalomyelitis and multiple sclerosis: lesion characterization with magnetization transfer imaging. Radiology 1992;182:483–491. [PubMed: 1732968]

Evangelou N, Esiri MM, Smith S, Palace J, Matthews PM. Quantitative pathological evidence for axonal loss in normal appearing white matter in multiple sclerosis. Ann Neurol 2000;47:391–395. [PubMed: 10716264]

Filippi M, Rocca MA. Magnetization transfer magnetic resonance imaging in the assessment of neurological diseases. J Neuroimaging 2004;14:303–313. [PubMed: 15358949]

Jiang H, van Zijl PC, Kim J, Pearlson GD, Mori S. DtiStudio: resource program for diffusion tensor computation and fiber bundle tracking. Comput Methods Programs Biomed 2006;81:106–116. [PubMed: 16413083]

Jones DK, Catani M, Pierpaoli C, Reeves SJ, Shergill SS, O'Sullivan M, Golesworthy P, McGuire P, Horsfield MA, Simmons A, Williams SC, Howard RJ. Age effects on diffusion tensor magnetic resonance imaging tractography measures of frontal cortex connections in schizophrenia. Hum Brain Mapp 2006;27:230–238. [PubMed: 16082656]

Jones DK, Griffin LD, Alexander DC, Catani M, Horsfield MA, Howard R, Williams SC. Spatial normalization and averaging of diffusion tensor MRI data sets. Neuroimage 2002;17:592–617. [PubMed: 12377137]

Kurtzke JF. Rating neurologic impairment in multiple sclerosis: an expanded disability status scale (EDSS). Neurology 1983;33:1444–1452. [PubMed: 6685237]

Lee MA, Blamire AM, Pendlebury S, Ho KH, Mills KR, Styles P, Palace J, Matthews PM. Axonal Injury or Loss in the Internal Capsule and Motor Impairment in Multiple Sclerosis. Arch Neurol 2000;57:65–70. [PubMed: 10634450]

Lin F, Yu C, Jiang T, Li K, Chan P. Diffusion Tensor Tractography-Based Group Mapping of the Pyramidal Tract in Relapsing-Remitting Multiple Sclerosis Patients. AJNR Am J Neuroradiol 2007;28:278–282. [PubMed: 17296994]

Lin F, Yu C, Jiang T, Li K, Li X, Qin W, Sun H, Chan P. Quantitative analysis along the pyramidal tract by length-normalized parameterization based on diffusion tensor tractography: application to patients with relapsing neuromyelitis optica. Neuroimage 2006;33:154–160. [PubMed: 16919971]

Loevner LA, Grossman RI, Cohen JA, Lexa FJ, Kessler D, Kolson DL. Microscopic disease in normal-appearing white matter on conventional MR images in patients with multiple sclerosis: assessment with magnetization-transfer measurements. Radiology 1995;196:511–515. [PubMed: 7617869]

Lucchinetti C, Bruck W, Parisi J, Scheithauer B, Rodriguez M, Lassmann H. Heterogeneity of multiple sclerosis lesions: implications for the pathogenesis of demyelination. Ann Neurol 2000;47:707–717. [PubMed: 10852536]

Mori S, Crain BJ, Chacko VP, van Zijl PC. Three-dimensional tracking of axonal projections in the brain by magnetic resonance imaging. Ann Neurol 1999;45:265–269. [PubMed: 9989633]

Mori S, van Zijl PC. Fiber tracking: principles and strategies - a technical review. NMR Biomed 2002;15:468–480. [PubMed: 12489096]

Mori, S.; Wakana, S.; van Zijl, PCM.; Nagae-Poetscher, LM. MRI Atlas of Human White Matter. Elsevier; Amsterdam: 2005.

Pagani E, Filippi M, Rocca MA, Horsfield MA. A method for obtaining tract-specific diffusion tensor MRI measurements in the presence of disease: application to patients with clinically isolated syndromes suggestive of multiple sclerosis. Neuroimage 2005;26:258–265. [PubMed: 15862226]

Pajevic S, Pierpaoli C. Color schemes to represent the orientation of anisotropic tissues from diffusion tensor data: application to white matter fiber tract mapping in the human brain. Magn Reson Med 1999;42:526–540. [PubMed: 10467297]

Partridge SC, Mukherjee P, Berman JI, Henry RG, Miller SP, Lu Y, Glenn OA, Ferriero DM, Barkovich AJ, Vigneron DB. Tractography-based quantitation of diffusion tensor imaging parameters in white matter tracts of preterm newborns. J Magn Reson Imaging 2005;22:467–474. [PubMed: 16161075]

Reich DS, Smith SA, Jones CK, Zackowski KM, van Zijl PC, Calabresi PA, Mori S. Quantitative characterization of the corticospinal tract at 3T. AJNR Am J Neuroradiol 2006;27:2168–2178. [PubMed: 17110689]

Rudick RA, Fisher E, Lee JC, Simon J, Jacobs L. Use of the brain parenchymal fraction to measure whole brain atrophy in relapsing-remitting MS. Multiple Sclerosis Collaborative Research Group. Neurology 1999;53:1698–1704. [PubMed: 10563615]

Schmierer K, Scaravilli F, Altmann DR, Barker GJ, Miller DH. Magnetization transfer ratio and myelin in postmortem multiple sclerosis brain. Ann Neurol 2004;56:407–415. [PubMed: 15349868]

Simon JH, Kinkel RP, Jacobs L, Bub L, Simonian N. A Wallerian degeneration pattern in patients at risk for MS. Neurology 2000;54:1155–1160. [PubMed: 10720290]

Smith SA, Farrell JAD, Jones CK, Reich DS, Calabresi PA, van Zijl PCM. Pulsed magnetization transfer imaging with body coil transmission at 3 Tesla: Feasibility and application. Magn Reson Med. 2006in press

Stieltjes B, Kaufmann WE, van Zijl PC, Fredericksen K, Pearlson GD, Solaiyappan M, Mori S. Diffusion tensor imaging and axonal tracking in the human brainstem. Neuroimage 2001;14:723–735. [PubMed: 11506544]

Tanabe JL, Vermathen M, Miller R, Gelinas D, Weiner MW, Rooney WD. Reduced MTR in the corticospinal tract and normal T2 in amyotrophic lateral sclerosis. Magnetic Resonance Imaging 1998;16:1163. [PubMed: 9858272]

Taylor JM, Cumberland WG, Meng X, Giorgi JV. Normal range estimation for repeated immunologic measures. Clin Diagn Lab Immunol 1996;3:139–142. [PubMed: 8991625]

Tievsky AL, Ptak T, Farkas J. Investigation of apparent diffusion coefficient and diffusion tensor anisotrophy in acute and chronic multiple sclerosis lesions. AJNR Am J Neuroradiol 1999;20:1491–1499. [PubMed: 10512236]

Toosy AT, Werring DJ, Orrell RW, Howard RS, King MD, Barker GJ, Miller DH, Thompson AJ. Diffusion tensor imaging detects corticospinal tract involvement at multiple levels in amyotrophic lateral sclerosis. J Neurol Neurosurg Psychiatry 2003;74:1250–1257. [PubMed: 12933929]

van Waesberghe JH, Kamphorst W, De Groot CJ, van Walderveen MA, Castelijns JA, Ravid R, Lycklama a Nijeholt GJ, van der Valk P, Polman CH, Thompson AJ, Barkhof F. Axonal loss in multiple sclerosis lesions: magnetic resonance imaging insights into substrates of disability. Ann Neurol 1999;46:747–754. [PubMed: 10553992]

Virta A, Barnett A, Pierpaoli C. Visualizing and characterizing white matter fiber structure and architecture in the human pyramidal tract using diffusion tensor MRI. Magn Reson Imaging 1999;17:1121–1133. [PubMed: 10499674]

Werring DJ, Clark CA, Barker GJ, Thompson AJ, Miller DH. Diffusion tensor imaging of lesions and normal-appearing white matter in multiple sclerosis. Neurology 1999;52:1626–1632. [PubMed: 10331689]

Werring DJ, Toosy AT, Clark CA, Parker GJ, Barker GJ, Miller DH, Thompson AJ. Diffusion tensor imaging can detect and quantify corticospinal tract degeneration after stroke. J Neurol Neurosurg Psychiatry 2000;69:269–272. [PubMed: 10896709]

Wilson M, Tench CR, Morgan PS, Blumhardt LD. Pyramidal tract mapping by diffusion tensor magnetic resonance imaging in multiple sclerosis: improving correlations with disability. J Neurol Neurosurg Psychiatry 2003;74:203–207. [PubMed: 12531950]

Woods RP, Cherry SR, Mazziotta JC. Rapid automated algorithm for aligning and reslicing PET images. J Comput Assist Tomogr 1992;16:620–633. [PubMed: 1629424]

Xu D, Mori S, Shen D, van Zijl PC, Davatzikos C. Spatial normalization of diffusion tensor fields. Magn Reson Med 2003;50:175–182. [PubMed: 12815692]

Xue R, van Zijl PC, Crain BJ, Solaiyappan M, Mori S. In vivo three-dimensional reconstruction of rat brain axonal projections by diffusion tensor imaging. Magn Reson Med 1999;42:1123–1127. [PubMed: 10571934]

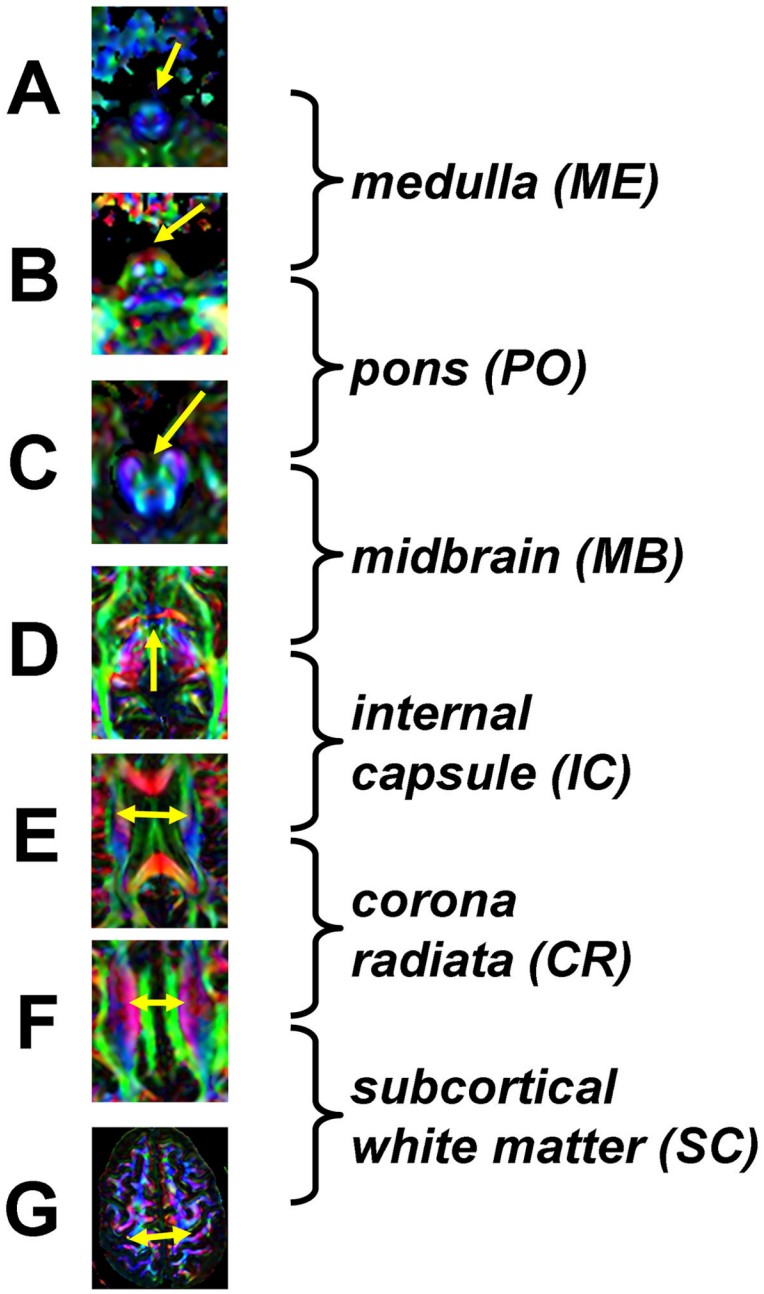

Figure 1.
Illustration of the boundary points used to demarcate segments of the corticospinal tracts. All boundary points are identified on axial slices from the principal eigenvector color maps, as shown. *A*, the most caudal slice in the medulla at which the pyramids first become distinct. *B*, the most caudal slice in the pons at which the anterior (transverse) fibers of the middle cerebellar peduncle first become evident. *C*, the most caudal slice in the midbrain at which those anterior fibers are no longer evident. *D*, the slice at which the anterior commissure is best seen crossing the midline. *E*, the most rostral slice at which both putamina are still visible. *F*, the most rostral slice at which transversely oriented fibers in the corpus callosum are still visible. *G*, the most rostral slice at which the characteristic “omega” shape of both central sulci

are still visible. The names given to the segments demarcated by these boundary points are shown in the figure; abbreviations are given for cross-referencing with Figures 2, 3, and 4.

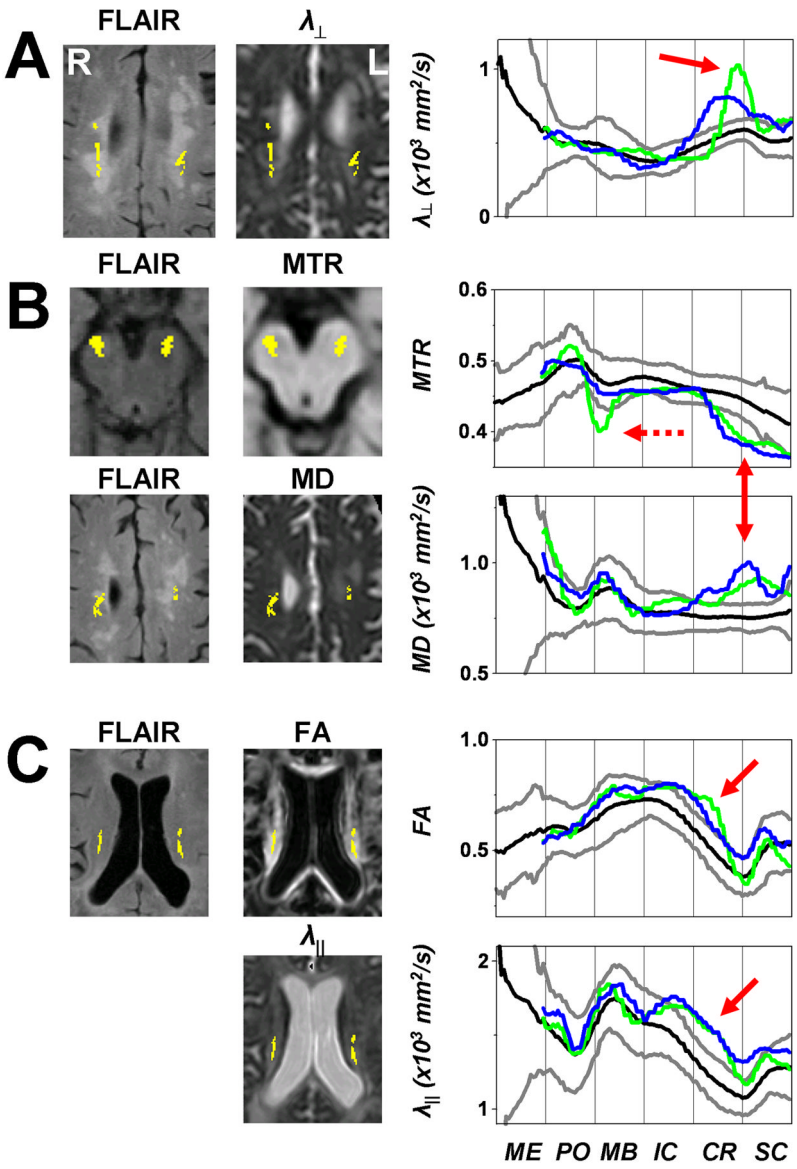

Figure 2.

Sample axial slices and tract profiles from 3 individuals with MS. *A*, 41-year-old woman with RRMS. *B*, 32-year-old woman with RRMS. C, 52-year-old man with PPMS. Each panel is organized as follows: *left column*, representative axial FLAIR image; *middle column*, representative axial image, at the same level, showing the MRI index map for which the corresponding tract profile is shown in the *right column*. In the images, the locations of the two CSTs are shown in yellow. The tract profiles on the right show the value of the listed MRI index as a function of normalized distance along the tract. The six segments of the CST defined in Figure 1 are demarcated by vertical lines: SC, subcortical white matter; CR, corona radiata; IC, internal capsule; MB, midbrain; PO, pons; ME, medulla. Solid black curves correspond to the mean across healthy controls; gray curves to 95% cutoffs showing the normal range; green curves to the right CST of the subject; and blue curves to the left CST of the subject. For these 3 individuals, only a portion of the medulla was imaged, so the medulla was not included in the tract profile analysis. Arrows point out features described in the text.

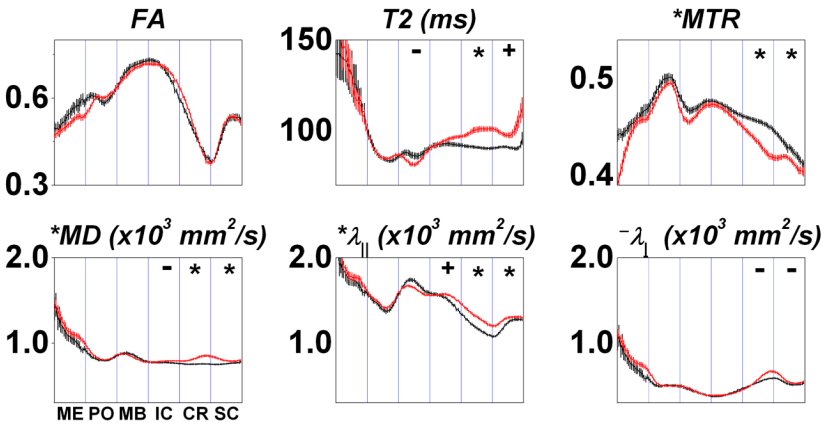

Figure 3.

CST profiles depicting the average MRI index at each tract position, averaged across healthy controls (black) and subjects with MS (red). Profiles are plotted against normalized distance along the CST. Error bars show one standard error of the mean in each tract subsegment. Significant differences are determined by partial correlation analysis, accounting for age, sex, and number of reconstructed fibers. Symbols located next to the panel title (whole tract) or above the curves in each tract segment denote different levels of significance: −, $p<0.05$; +, $p<0.01$; *, $p<0.001$. Segment abbreviations are as in Figures 1 and 2.

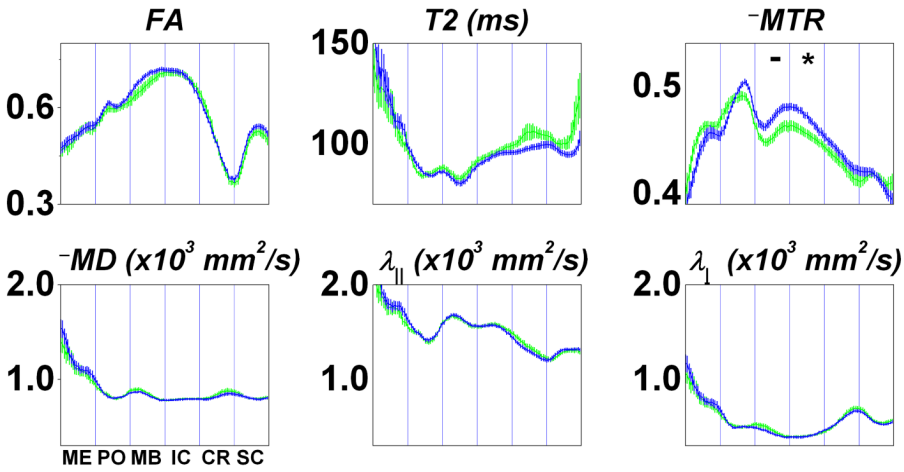

Figure 4.
CST profiles depicting the average MRI index at each tract position, averaged across subjects with relapsing remitting MS (blue) and secondary progressive MS (green). The format follows that of Figure 3.

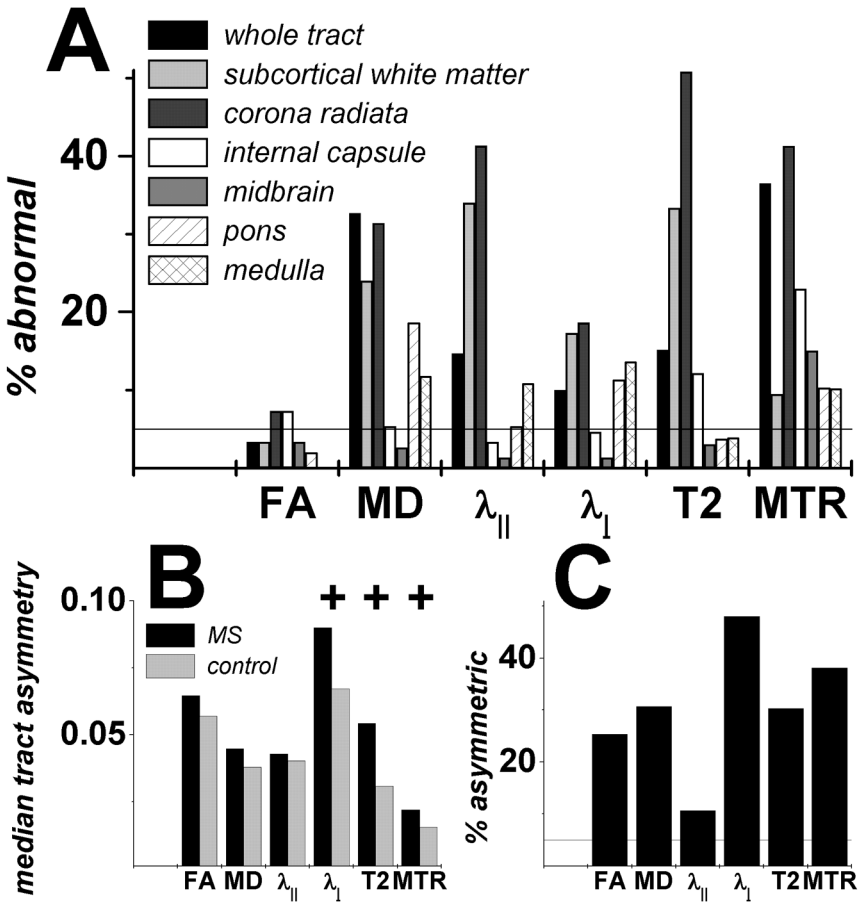

Figure 5.

A, percentage of individuals with MS who had significantly abnormal MRI indices for the whole CST and each component segment. Abnormality was determined relative to the distribution of indices in healthy controls, without correction for age, sex, and number of reconstructed fibers. The horizontal line at 5% denotes the percentage of abnormal indices expected by chance. *B*, total tract asymmetry index, which can range from 0 (no asymmetry) to 1 (maximal asymmetry), for each MRI index. Symbols (+) above the columns denote significant differences of $p<0.01$, determined as described in Methods. *C*, percentage of individuals with MS who had significantly asymmetric MRI indices across the whole CST.